# Decoherence, entanglement, and chaos in the Dicke model

Xi-Wen Hou[1,2] and Bambi Hu[1,3]
[1]*Department of Physics and Centre for Nonlinear Studies, Hong Kong Baptist University, Hong Kong, China*
[2]*Department of Physics, Huazhong Normal University, Wuhan 430079, China*
[3]*Department of Physics, University of Houston, Houston, Texas 77204, USA*
(Received 20 October 2003; published 23 April 2004)

The dynamical properties of quantum entanglement in the Dicke model without rotating-wave approximation are investigated in terms of the reduced-density linear entropy. The characteristic time of decoherence process in the early-time evolution is numerically obtained and it is shown that the characteristic time decreases as the coupling parameter increases. The mean entanglement, which is defined to be averaged over time, is employed to describe the influences of both quantum phase transition and corresponding classical chaos on the behavior of entanglement. For a given energy, initial conditions are taken to be minimum uncertainty wave packets centered at regular and chaotic regions of the classical phase space. It is shown that the entanglement has a distinct change at the quantum phase transition, and that the entanglement for regular initial conditions is smaller than that for chaotic ones in the case of weak coupling, while it fluctuates with small amplitude in strong coupling and for chaotic initial conditions.

DOI: 10.1103/PhysRevA.69.042110 PACS number(s): 03.65.Ud, 05.45.Mt, 73.43.Nq

## I. INTRODUCTION

In recent years, entanglement has been extensively studied since it has been recognized as a quantum resource for quantum computation [1], quantum dense coding [2], quantum teleportation [3], and quantum secret protocols [4]. Although the definition of entanglement itself is not of dynamical nature, entangled states are often generated dynamically; that is, even if subsystems are not entangled initially, the interaction between them produces entanglement in the system as time evolves. This is an important dynamical origin of decoherence. Consequently, a lot of work has been devoted to understanding decoherence, dynamics of quantum entanglement, quantum chaos, and quantum phase transitions. For example, an approximate but very simple classical theory of linear entropy production of intrinsic decoherence dynamics associated with localized initial states was derived for smooth Hamiltonian systems [5], indicating that the rate of entropy production is closely related to the stability properties of classical trajectories, and that the small-amplitude oscillations of entropy may be regarded as fingerprints of the underlying classical chaos. For an open quantum system the entropy production rate could be used as a diagnostic for quantum chaos [6]. In general, chaotic systems tend to produce larger entanglement than the regular systems. However, exceptions for classically regular systems are found in Ref. [7]. Furthermore, since quantum entanglement is responsible for the appearance of long-range correlations, it is expected to play a crucial role in the study of quantum phase transitions (QPT). It is demonstrated that the entanglement is maximum for the parameter values corresponding roughly to a bifurcation of a fixed point in the corresponding semiclassical dynamics in a driven dissipative quantum system [8]. A similar property also exists in the *XY* spin chain [9], where one- and two-spin entanglement measures are employed, while the entanglement between a block $L$ contiguity and the rest of the chain at the critical point displays a logarithmic divergence for large $L$ [10]. These mean that the entanglement behavior near and at the QPT depends on the measure of entanglement and the studied model. Therefore, it will be very interesting to further understand these properties of entanglement for other systems. In the present paper, we study the Dicke model (DM) without rotating-wave approximation (RWA), investigating how the quantum entanglement depends on the coupling parameter that describes the interaction between atoms and radiation field. Thereby the decoherence, the classical chaos, and the QPT are discussed.

Since the pioneering work of Dicke [11] on cooperative spontaneous emission, much attention has been paid to the interaction of the radiation field with a collection of two-level atoms located within a distance much smaller than the wavelength of the radiation. Such a system is commonly referred to as Dicke model, which is usually considered in the RWA when the atom-field coupling strength is weak. This makes the DM integrable, simplifying the analysis of some important phenomena such as super-radiance, collapses, and revivals of Rabi oscillations, squeezing, and phase transition [12]. Recently, the DM has been extensively studied without RWA, with its quantum-chaotic properties being discussed by several authors [13] without being connected with the QPT. This case has been very recently investigated by Emary and Brandes [14] by numerically analyzing the level statistics. They have demonstrated that the DM undergoes a transition from quasi-integrability to quantum chaotic and that this transition is caused by the precursors of QPT. However, the dynamical entanglement near and at QPT has not yet been studied. Although Furuya *et al.* [15] studied entanglement process in a varied version of DM and concluded that for short times there is a faster increase in decoherence for the chaotic initial conditions as compared to regular ones, which have oscillatory increase, the impact of QPT on entanglement and how the decoherence depends on the coupling parameter were not discussed. In this work, we study the dynamical entanglement that is quantitatively expressed in terms of the reduced-density linear entropy, with the varied couplings in DM. When the initial state is taken to be the

 

ground state without the interaction between the atoms and the field, we are able to investigate the characteristic time of the decoherence and the entanglement properties with different numbers of atoms with the coupling parameter that covers the QPT point.

We also study the behavior of entanglement dynamics with different initial states, assuming the coupling parameter fixed. For a given energy, initial states are prepared as minimum uncertainty wave packets placed at regular and chaotic regions of the classical phase space. Therefore, the influence of chaos on the entanglement will be explored.

The paper is organized as follows. Section II introduces the Dicke model, and its classical version and classical bifurcation are derived in terms of coherent state theory. In Sec. III, the characteristic time of decoherent process in the early-time evolution is numerically obtained with the coupling parameter. The mean entanglement, which is defined to be averaged over time, is used to study the relations between the entanglement and the quantum phase transition, and between the entanglement and the classical chaos. Conclusion is given in Sec. IV.

## II. THE DICKE MODEL

We consider the Dicke model that describes a collection of $N$ two-level atoms interacting with a single-mode radiation field via a dipole interaction with an atom-field coupling parameter $\lambda$. The Dicke Hamiltonian without rotating-wave approximation is written as ($\hbar=1$ hereafter)

$$H=\omega_0 J_z+\omega a^\dagger a+\frac{\lambda}{\sqrt{2j}}(a^\dagger+a)(J_++J_-), \tag{1}$$

where $\omega_0$ and $\omega$ are the splitting of $N$ two-level atoms and the frequency of a single bosonic mode, respectively, $J_z$ is the operator of atomic inversion, $a$ and $a^\dagger$ are the annihilation and creation operators of the field mode, $j$ is the length of the collective spin operators, and $J_+$ and $J_-$ are the collective atomic raising and lowing operators. They satisfy the su(2) Lie algebra:

$$[J_+,J_-]=2J_z,\quad [J_z,J_\pm]=\pm J_\pm. \tag{2}$$

The Hilbert space of this algebra is spanned by the Dicke states $|j,m\rangle$ ($m=-j,-j+1,\ldots,j-1,j$), which are the eigenstates of $J^2$ and $J_z$ with the eigenvalues $j(j+1)$ and $m$. The raising and lowering operators act on these states as $J_\pm|j,m\rangle=\sqrt{j(j+1)-m(m\pm1)}|j,m\pm1\rangle$. Note that, in general, the set of atomic configurations for $N>2$ is nontrivial [16], and the states are nonseparable and have entanglement [17] in terms of the individual atom configurations. In this work, we also take $j$ to be its maximal value $j=N/2$ as done in Refs. [14,15].

The Hamiltonian (1) has a conserved parity $\Pi=\exp[i\pi(a^\dagger a+J_z+j)]$ with the eigenvalues $\pm1$. An interesting physical realization of the Hamiltonian (1) is given by the coupling of the internal levels of atoms or ions to a mode of their quantized oscillatory motion in a harmonic trap [18]. Recently, reversible entanglement of ions has been proposed [19], and the experimental realizations have been reported in the cases of several ions [20].

Once the quantum Hamiltonian (1) is at hand, we are able to study its entanglement dynamics. Before doing that, one must choose initial quantum states. Most works have taken the initial states to be the ground states under considered quantum systems, and then ground-state entanglement is analyzed [8–10,21,22]. In our case, we take the initial states to be coherent states, namely, minimum uncertainty wave packets centered in the corresponding classical phase space. That allows us to explore the relation between the entanglement and classical chaos. The initial quantum states chosen in the present study are as follows:

$$|\psi(0)\rangle=|\tau\rangle\otimes|\beta\rangle\equiv|\tau\beta\rangle, \tag{3}$$

where $|\tau\rangle(|\beta\rangle)$ are the atomic (field-) coherent states given by [23]

$$|\tau\rangle=(1+\tau\tau^*)^{-j}e^{\tau J_+}|j,-j\rangle,$$

$$|\beta\rangle=e^{-\beta\beta^*/2}e^{\beta a^\dagger}|0\rangle, \tag{4}$$

where

$$\tau=\frac{q_1+ip_1}{\sqrt{4j-(q_1^2+p_1^2)}},$$

$$\beta=\frac{1}{\sqrt{2}}(q_2+ip_2), \tag{5}$$

$|0\rangle$ is the bosonic field ground state, and $q_1,p_1,q_2,p_2$ describe the phase space of the system under consideration with indices 1 and 2 for the atomic and field subsystem, respectively. Thus the classical Hamiltonian corresponding to Eq. (1) can be obtained by a standard procedure as [23]

$$\begin{aligned}H_{cl}&\equiv\langle\tau\beta|H|\tau\beta\rangle\\&=\frac{\omega_0}{2}(q_1^2+p_1^2-2j)+\frac{\omega}{2}(q_2^2+p_2^2)\\&\quad+2\lambda\sqrt{\frac{4j-q_1^2-p_1^2}{4j}}q_1q_2,\end{aligned} \tag{6}$$

then the corresponding Hamilton's equations of motion are given by

$$\dot q_1=\omega_0p_1-2\lambda\frac{p_1q_1q_2}{\sqrt{4j(4j-q_1^2-p_1^2)}},$$

$$\dot q_2=\omega p_2,$$

$$\dot p_1=-\omega_0q_1-2\lambda q_2\sqrt{\frac{4j-q_1^2-p_1^2}{4j}}+2\lambda\frac{q_1^2q_2}{\sqrt{4j(4j-q_1^2-p_1^2)}},$$

$$\dot p_2=-\omega q_2-2\lambda q_1\sqrt{\frac{4j-q_1^2-p_1^2}{4j}}. \tag{7}$$

We now determine the fixed points in the classical phase space $(q_1,p_1,q_2,p_2)$ by setting $\dot{q}_1=\dot{q}_2=\dot{p}_1=\dot{p}_2=0$. The simplest fixed point is given by $q_1=q_2=p_1=p_2=0$, the coordinate origin. By calculating the Hessian stability matrix from the second derivatives of $H_{cl}$, we see that this fixed point is only stable when

$$\omega_0^2+\omega^2-\sqrt{(\omega_0^2-\omega^2)^2+16\lambda^2\omega_0\omega}>0, \tag{8}$$

i.e., when $\lambda<\sqrt{\omega_0\omega}/2=\lambda_c$. There are two other fixed points, both of which have $p_1=p_2=0$, with $q_1$ and $q_2$ given by

$$q_1=\pm\sqrt{2j\left(1-\frac{\lambda_c^2}{\lambda^2}\right)},$$

$$q_2=\mp\frac{2\lambda}{\omega}\sqrt{j\left(1-\frac{\lambda_c^4}{\lambda^4}\right)}. \tag{9}$$

These two quantities only remain real and stable provided that $\lambda>\lambda_c$. So, below the coupling $\lambda_c$, only one fixed point exists, which lies at the coordinate's origin and is stable. Above $\lambda_c$, this fixed point becomes unstable and two new stable fixed points appear at the coordinates $(-q_1,+q_2)$ and $(+q_1,-q_2)$ given by Eq. (9) with $p_1=p_2=0$.

The above obtained classical bifurcation point at $\lambda_c$ corresponds to the quantum phase transition [14] by the exact Holstein-Primakoff transformation of the Hamiltonian (1) in the thermodynamics limit $N\to\infty$. It is demonstrated that the quantum phase transition is the second-order one and quantum chaos is triggered by precursors of this transition by in-detail investigations of the ground-state energy and wave function, and the nearest-neighbor level-spacing distribution [14]. In the following section, the behavior of entanglement dynamics is studied with the several different values of $N$.

## III. THE ENTANGLEMENT DYNAMICS

Several measures of quantum entanglement have been proposed. These include entanglement of formation [24], entanglement of distillation [25], relative entropy of entanglement [26], linear entropy of entanglement [27], concurrence [28], negativity [29], and so on. In our case the entanglement can be described by the linear entropy or the von Neumann entropy. We calculate the linear entropy and the von Neumann entropy, and the similar behavior of the two measures is found. Thus we only present the results of the linear entropy. Furthermore, the linear entropy is extensively used in the study of decoherence [5,6,8,9,30–34]. It is important that the characteristic time of decoherence [33] can be obtained in the calculation of the linear entropy.

The linear entropy of entanglement is defined as [27]

$$S(t)=1-\mathrm{Tr}_1\rho_1(t)^2, \tag{10}$$

where $\mathrm{Tr}_1$ denotes a trace over the first subsystem, and $\rho_1(t)$ is the reduced-density matrix, $\rho_1(t)=\mathrm{Tr}_2|\psi(t)\rangle\langle\psi(t)|$, where indices 1 and 2 stand for the atomic and field subsystem, and $|\psi(t)\rangle$ is the quantum state of the full system, which evolves in time under the action of Hamiltonian (1). The quantity $S(t)$ describes the degree of purity of the subsystem in a scale from 0 (pure state) to 1 (statistical mixture). It also describes the degree of decoherence [5]. Thus in this section we discuss (i) the characteristic time of decoherence, (ii) the influence of the quantum phase transition on the entanglement, and (iii) the relation between the entanglement and classical chaos.

### A. The characteristic time of decoherence

The physics of decoherence has been extensively studied during the last few years both from the theoretical and also from the experimental point of view. As part of these studies it has been recognized that the docoherence process has rather unique properties for systems whose classical analogs are chaotic. Reference [6] suggested that entropy production rate during decoherence could be used as a diagnostic for quantum chaos in open quantum system. The quantum-classical correspondence between classical and quantum descriptions of dynamics of decoherence was studied for smooth Hamiltonian systems [5], where the classicality of early-time decoherence dynamics was described using second-order perturbative treatment. It is now understood that the decoherence is closely related to the nonlinear parameter describing interactions [30]. Thus it is important to look for the characteristic time of decoherence upon variance of the coupling parameter. In particular, it becomes very interesting if the quantum systems have a quantum phase transition.

Most works on decoherence have focused on using second-order perturbative treatment [5,30,31] and the interaction of the quantum system with its environment that has many degrees of freedom [30,32,33]. A latest important work has shown that decoherence of the center-of-mass motion of a composed system can occur through the entanglement of its own subsystems with even a few degrees of freedom due to the chaotic nature of internal dynamics [34]. However, to our best knowledge, how the characteristic time of decoherence depends on the model parameter has not yet been discussed. We have determined the characteristic time $t_d$ for the DM, which is defined as the instant when the slope of the curve of the entropy $S(t)$ decreases appreciably in the early-time evolution [33], that is, $t_d$ is determined by setting $dS(t)/dt|_{t=td}=0$.

The characteristic time $t_d$ of the decoherence process is calculated in the resonant case, $\omega=\omega_0=1$, with the initial state, for simplicity, being taken to be the ground state without the coupling between the atoms and the field. Figure 1 shows the characteristic time $t_d$ of decoherence vs the model parameter $\lambda$ with several numbers of atoms, $N=1,2,3,9,25$, where $\lambda$ is changed from 0.001 to 1. A number of observations are in order. First, the characteristic time $t_d$ decreases as the coupling parameter $\lambda$ increases. Second, if $\lambda$ is less than 0.08, $t_d$ is almost the same for different number of atoms. The curves $t_d$ for $N=9$ and 25 have a little difference compared with those for small number of atoms, $N=1,2,3$. Finally, and most importantly, all the curves $t_d$ do not have any distinct change near and at the critical point $\lambda_c=0.5$. It is straightforward to get the similar curves for

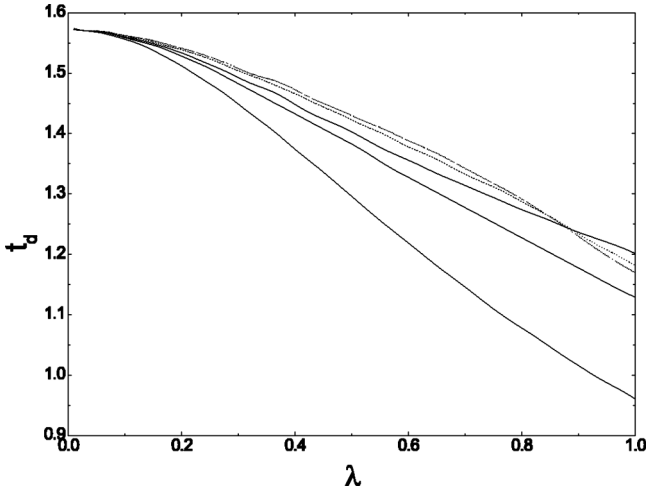


FIG. 1. The dependence of the characteristic time $t_d$ (in scaled unit) of decoherence process in the early-time evolution on the coupling parameter λ. The solid curves from bottom to top are for $N=1$, 2, 3, and dashed and dotted curves for $N=9$ and 25, respectively, where $N$ is the number of atoms in the Dicke model. Here there is no obvious change at the critical coupling $\lambda_c=0.5$ with $\omega=\omega_0=1$.

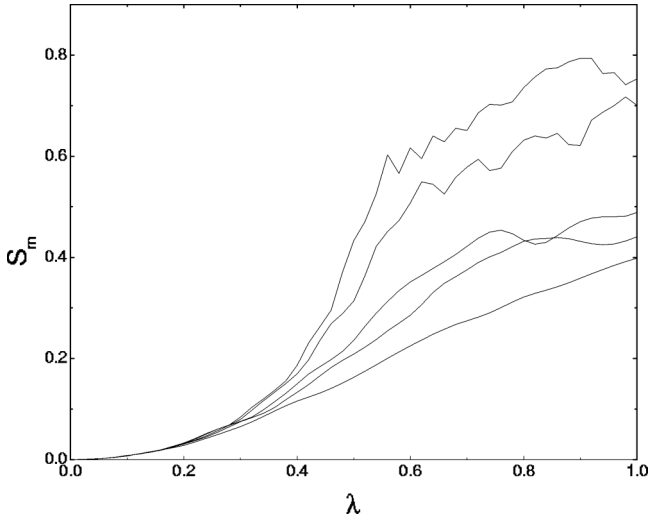


FIG. 2. The dependence of the mean entanglement $S_m$ on the coupling parameter λ. The curves from bottom to top are for $N=1$, 2, 3, 9, 25, respectively. A distinct change at the critical point $\lambda_c=0.5$ is nicely observed for $N=9$, 25 with $\omega=\omega_0=1$.

large coupling parameter and the large number of atoms in the model.

### B. The entanglement near and at the quantum phase transition

Investigations of the behaviors of entanglement near and at the quantum phase transition have been so far restricted to interacting-1/2 systems on a one-dimensional lattice [9,10,35] or on a simplex [36], which requires the more or less artificial splitting into two-spin subsystems. It is shown that the entanglement measured by the von Neumann entropy or the pairwise concurrence is largest near quantum critical points. This is also demonstrated by the latest studies of the entanglement between a qubit and the environment in the spin-boson model [21] and the entanglement between atoms and field in the Dicke model [22]. Those works, however, focused solely on static properties of the entanglement. In this section, we explore the behavior of entanglement dynamics near and at the quantum phase transition. To this end, we introduce the mean entanglement $S_m$, which is defined by

$$S_m = \frac{1}{T}\int_0^T S(t)dt, \tag{11}$$

where $T$ is the total time of evolution, which is taken to be 20 in scaled unit in the resonant case $(\omega=\omega_0=1)$ hereafter.

Figure 2 shows that the mean entanglement $S_m$ varies with the coupling parameter λ, where the number of atoms $N$ is taken to be 1, 2, 3, 9, and 25, for example, and the initial state is also taken to be the ground state without the coupling between the atoms and the field for simplicity. Some important properties are observed in Fig. 2. First, the mean entanglement $S_m$ increases as the number of atoms increases. The increasing quantity above the critical point $(\lambda_c=0.5)$ is larger than that below the critical point. The mean entanglement also increases with coupling strength λ, but it saturates after a certain magnitude of coupling strength that will be seen to roughly correspond to the emergence of complete classical chaos in the following section. This observation agrees with that for coupled standard maps [37]. Furthermore, the mean entanglement above the critical point fluctuates in small amplitude with the coupling parameter λ, whose frequency increases with the number of atoms. This may also be regarded as a fingerprint of the underlying quantum chaos [5] that was demonstrated in Ref. [14]. Finally, the mean entanglement $S_m$ has more distinct change at the quantum critical point $(\lambda_c=0.5)$ for the larger number of atoms. This relation between the entanglement and the number of atoms agrees with that obtained in Ref. [22], where the ground-state static entanglement measured by concurrence is maximum exactly at the critical point when the number of atoms is infinity. The different measures of entanglement for mixed quantum states are referred to Ref. [38].

### C. The relation between entanglement and classical chaos

The relation between entanglement and classical chaos has been previously studied with the example of a varied Dicke model [15]. It was found that the entanglement rate is considerably enhanced if the initial wave packet is placed in a chaotic region. Such rates have been related to classical Lyapunov exponents with the help of a coupled kicked top model [39]. It is shown that the increment in the strength of chaos does not enhance the production rate of entanglement when the coupling is weak enough and the kicked tops are strongly chaotic [40]. Another work of similar kind has been done for coupled standard maps [37]. In this section we extend such a study to the Dicke model.

We numerically integrate Hamilton's equations of motion (7) for a variety of parameters and initial conditions. In order to analyze classical chaos resulting from these integrations,

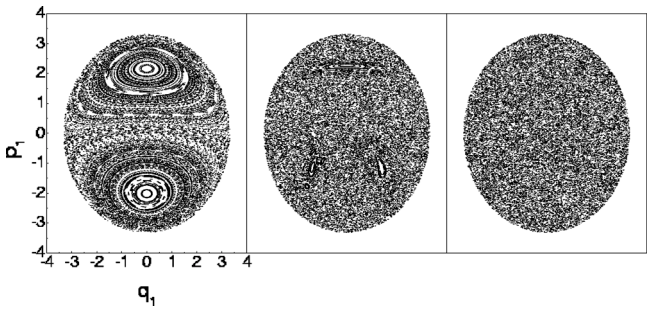


FIG. 3. Poincaré sections for the classical Dicke model for three increasing couplings, $\lambda=0.1$, 0.5, 0.9 (from left to right), with $N=9$ and $E=1$. The Hamiltonian is on scaled resonance $\omega=\omega_0=1$.

we employ Poincaré sections through the four-dimensional phase space. As this system is Hamiltonian, the energy

$$E=\frac{\omega_0}{2}(q_1^2+p_1^2-2j)+\frac{\omega}{2}(q_2^2+p_2^2)+2\lambda\sqrt{\frac{4j-q_1^2-p_1^2}{4j}}q_1q_2 \tag{12}$$

is conserved, and thus we define our surface of section by $q_2=0$ with $p_1$ being fixed by the energy $E$. We only record traversals for $p_2>0$. Poincaré sections for illustrative parameter values are shown in Fig. 3. At low $\lambda$ ($\lambda=0.1$), the Poincaré section consists of a series of regular, periodic orbits and irregular orbits. Approaching to the critical coupling ($\lambda=0.5$), we see a change in the character of the periodic orbits, and also the emergence of a number of chaotic trajectories. Increasing the coupling further results in the breakup of the remaining periodic orbits and the whole phase space becomes chaotic for coupling a little over the critical value. The section at $\lambda=0.9$ is given as an example.

We now determine behaviors of the mean entanglement with different initial states that are taken to be coherent states placed at the corresponding classical phase space. For comparison, we take the coherent states constructed from the points in the straight line at $q_1=0$ at the three sections (Fig. 3). Thus the initial states are only determined by the values of $p_1$. Figure 4 shows that the mean entanglement $S_m$ varies with $p_1$ for the corresponding sections. Some observations in Fig. 4 are the following. For the weak coupling ($\lambda=0.1$), the regular, periodic orbits produce smaller mean entanglement than the irregular orbits. For the critical coupling ($\lambda=0.5$), the mean entanglement fluctuates with $p_1$ in small amplitude, and the smallest mean entanglement almost corresponds to the regular orbits at $p_1=3.0$ in the island in the section since the chaotic orbits occupy most of the classical phase space. For the strong coupling ($\lambda=0.9$), the mean entanglement also fluctuates with $p_1$ with the smaller amplitude, and the smallest mean entanglement remains at $p_1=3.0$, but here the orbits are chaotic. Hence, the conclusion that the chaotic regime tends to produce larger entanglement than the regular regime [15,37] is also applicable to the Dicke model only in the weak coupling. Finally, we notice that the mean entanglement at the border of the sections also has a larger value than that at the regular orbits. This therefore appears to be a border effect.

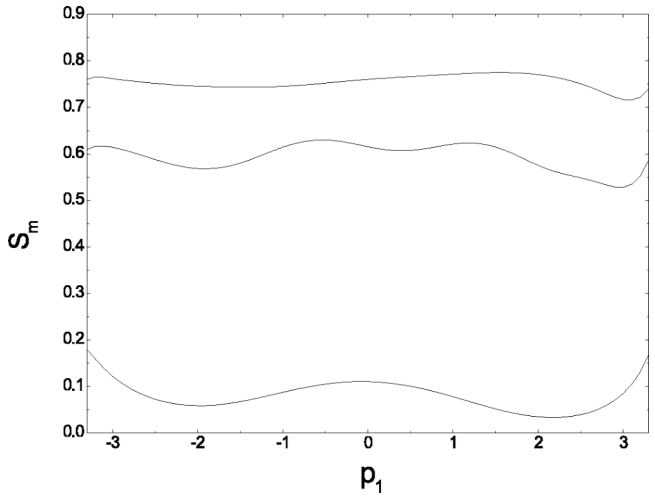


FIG. 4. The dependence of the mean entanglement $S_m$ on the initial coherent states characterized by one of the classical variables $p_1$, corresponding to the straight line at $q_1=0$ in Poincaré sections in Fig. 3. The curves from bottom to top are for $\lambda=0.1$, 0.5, 0.9 respectively.

## IV. CONCLUSION

We have studied the entanglement dynamics in the Dicke model without rotating-wave approximation with varied coupling parameter and initial quantum states. The entanglement is measured by the reduced-linear density entropy. The characteristic time of decoherent process in the early-time evolution is numerically obtained from the linear entropy. It is found that the characteristic time decreases as the coupling parameter increases when the initial state is taken to be the ground state without coupling between atoms and field. An obvious variance of the characteristic time at the critical coupling is not observed in our study.

The mean entanglement averaged over time has been used for the description of behaviors of entanglement dynamics with varied coupling parameter, number of atoms, and initial conditions. Therefore, the influence of quantum phase transition and the classical chaos on the entanglement has been explored. It is shown that the larger the number of atoms in the model, the more distinct is the change the mean entanglement at the critical coupling. It is also shown that the mean entanglement increases with the coupling parameter and the number of atoms in the model, but it fluctuates around its saturation value when the coupling parameter or the initial state is in classical chaotic regime. This saturation value depends on the number of atoms, coupling parameter, initial conditions, total time of evolution, and so on. It is difficult to get its analyzed expression in general. Nevertheless, the saturation value remains between 0 and 1. When the coherent state placed at the corresponding classical phase

space is taken as an initial state, it is found that the mean entanglement for a regular orbit is smaller than that for an irregular one in the case of weak coupling.

It is desirable to investigate the dynamical properties with other measures of entanglement for comparison. It is possible to study a similar entanglement behavior in other models and results will be discussed elsewhere.

**ACKNOWLEDGMENTS**

We would like to thank the members at the Centre for Nonlinear Studies of Hong Kong Baptist University for valuable discussions. This work was supported in part by the grants from the Hong Kong Research Grants Council (RGC) and the Hong Kong Baptist University Faculty Research Grant (FRG).

[1] S. Loyd, Science **261**, 1589 (1993).
[2] C. H. Bennett and S. Wiesner, Phys. Rev. Lett. **69**, 2881 (1992).
[3] C. H. Bennett, G. Brassard, C. Crépeau, R. Jozsa, A. Peres, and W. K. Wooters, Phys. Rev. Lett. **70**, 1895 (1993).
[4] R. Cleve, D. Gottesman, and H. Lo, Phys. Rev. Lett. **83**, 1874 (1999).
[5] J. Gong and P. Brumer, Phys. Rev. A **68**, 022101 (2003).
[6] W. H. Zurek and J. P. Paz, Physica D **83**, 300 (1995); D. Monteoliva and J. P. Paz, Phys. Rev. Lett. **85**, 3373 (2000).
[7] A. Tanaka, J. Phys. A **29**, 5475 (1996); R. M. Angelo, K. Furuyu, M. C. Nemes, and G. Q. Pellegrino, Phys. Rev. E **60**, 5407 (1999).
[8] S. Schneider and G. J. Milburn, Phys. Rev. A **65**, 042107 (2002).
[9] T. J. Osborne and M. A. Nilsen, Phys. Rev. A **66**, 032110 (2002).
[10] G. Vidal, J. I. Latorre, E. Rico, and A. Kitaev, Phys. Rev. Lett. **90**, 227902 (2003).
[11] R. H. Dicke, Phys. Rev. **93**, 99 (1954).
[12] C. Leonardi, F. Persico, and G. Vetri, Riv. Nuovo Cimento **9**, 1 (1986); B. W. Shore and P. L. Knight, J. Mod. Opt. **40**, 1195 (1993); G. Ramon, C. Brif, and A. Mann, Phys. Rev. A **58**, 2506 (1998).
[13] M. Kús, Phys. Rev. Lett. **54**, 1343 (1983); R. Graham and M. Höhnerbach, *ibid.* **57**, 1378 (1986); L. Müller, J. Stolze, H. Leschke, and P. Nagel, Phys. Rev. A **44**, 1022 (1991); G. A. Finney and J. Gea-Banacloche, Phys. Rev. E **54**, 1449 (1996).
[14] C. Emary and T. Brandes, Phys. Rev. Lett. **90**, 044101 (2003); Phys. Rev. E **67**, 066203 (2003).
[15] K. Furuya, M. C. Nemes, and G. Q. Pellegrino, Phys. Rev. Lett. **80**, 5524 (1998); R. M. Angelo, K. Furuya, M. C. Nemes, and G. Q. Pellegrino, Phys. Rev. A **64**, 043801 (2001).
[16] F. T. Arrechi, E. Courtens, R. Golmore, and H. Thomas, Phys. Rev. A **6**, 2211 (1972).
[17] X. Wang and K. Mølmer, Eur. Phys. J. D **18**, 385 (2002).
[18] D. J. Wineland, J. J. Bollinger, W. M. Itano, and D. J. Heinzen, Phys. Rev. A **50**, 67 (1994).
[19] K. Mølmer and A. Sørensen, Phys. Rev. Lett. **82**, 1835 (1999); A. Sørensen and K. Mølmer, Phys. Rev. A **62**, 022311 (2000).
[20] Q. A. Turchette, C. S. Wood, B. E. King, C. J. Myatt, D. Leibfried, W. M. Itano, C. Monroe, and D. J. Wineland, Phys. Rev. Lett. **81**, 3631 (1998); Ch. Roos, Th. Zeiger, H. Rohde, H. C. Nägerl, J. Eschner, D. Leibfried, F. Schmidt-Kaler, and R. Blatt, *ibid.* **83**, 4713 (1999).
[21] T. A. Costi and R. H. McKenzie, Phys. Rev. A **68**, 034301 (2003).
[22] N. Lambert, C. Emary, and T. Branders, Phys. Rev. Lett. **92**, 073602 (2004).
[23] W. M. Zhang, D. H. Feng, and R. Gilmore, Rev. Mod. Phys. **62**, 867 (1990).
[24] C. H. Bennett, D. P. DiVincenzo, J. A. Smolin, and W. K. Wooters, Phys. Rev. A **54**, 3824 (1996).
[25] C. H. Bennett, G. Brassard, S. Popescu, B. Schumacher, J. Smolin, and W. K. Wooters, Phys. Rev. Lett. **76**, 722 (1996).
[26] V. Vedral, M. B. Plenio, K. Jacobs, and P. L. Knight, Phys. Rev. A **56**, 4452 (1997); V. Vedral, M. B. Plenio, M. A. Rippin, and P. L. Knight, Phys. Rev. Lett. **78**, 2275 (1997).
[27] C. H. Bennett, H. J. Bernstein, S. Popescu, and B. Schumacher, Phys. Rev. A **53**, 2046 (1996).
[28] S. Hill and W. K. Wooters, Phys. Rev. Lett. **78**, 5022 (1997).
[29] K. Zyczkowski, P. Horodecki, A. Sanpera, and M. Lewenstein, Phys. Rev. A **58**, 883 (1998).
[30] W. H. Zurek, Rev. Mod. Phys. **75**, 715 (2003).
[31] J. I. Kim, M. C. Nemes, A. F. R. de Toledo Piza, and H. E. Borges, Phys. Rev. Lett. **77**, 207 (1996).
[32] W. H. Zurek, S. Habib, and J. P. Paz, Phys. Rev. Lett. **70**, 1187 (1993).
[33] P. Földi, A. Czirjaák, and M. G. Benedict, Phys. Rev. A **63**, 033807 (2001); P. Földi, M. G. Benedict, A. Czirják, and B. Molnár, *ibid.* **67**, 032104 (2003).
[34] H. K. Park and S. W. Kim, Phys. Rev. A **67**, 060102(R) (2003).
[35] J. L. Latorre, E. Rico, and G. Vidal, e-print quant-ph/0304098.
[36] J. Vadal, G. Palacois, and R. Mosseri, e-print cond-mat/0305573.
[37] A. Lakshminarayan, Phys. Rev. E **64**, 036207 (2001).
[38] T. C. Wei, K. Nemoto, P. M. Goldbart, P. G. Kwiat, W. J. Munro, and F. Verstraete, Phys. Rev. A **67**, 022110 (2003).
[39] P. A. Miller and S. Sarkar, Phys. Rev. E **60**, 1542 (1999).
[40] H. Fujisaki, T. Miyadera, and A. Tanaka, Phys. Rev. E **67**, 066201 (2003).